Deconvolution Techniques in Time-Domain and Fourier-Domain Optical Coherence Tomography

Lévesque, D.; Vergnole, S.; Dufour, M. L.; Gauthier, B.; Lamouche, G.

Proceedings of the 34th Annual Review of Progress in Quantitative Nondestructive Evaluation, 2007., 2007-07-27

DECONVOLUTION TECHNIQUES IN TIME-DOMAIN AND FOURIER-DOMAIN OPTICAL COHERENCE TOMOGRAPHY

D. Lévesque, S. Vergnole, M. L. Dufour, B. Gauthier, and G. Lamouche

Industrial Materials Institute, National Research Council Canada, Boucherville, Quebec, Canada

ABSTRACT. The imaging resolution in optical coherence tomography can be improved by using deconvolution techniques. Both the Time-Domain OCT (TD-OCT) and the Fourier-Domain OCT (FD-OCT) are considered. A deconvolution technique based on Wiener filtering and autoregressive spectral extrapolation (ASE) allows a resolution enhancement by a factor of 4 in TD-OCT and of 2 in FD-OCT. The performance of both approaches is evaluated from TD and FD-OCT measurements of the thickness of the upper epoxy layer of a carbon-epoxy composite.

Keywords: TD-OCT, FD-OCT, Deconvolution, Resolution
PACS: 07.05.Pj, 42.25.Hz, 42.30.Kq, 42.30.Va, 42.62.Cf

INTRODUCTION

Optical Coherence Tomography (OCT) is now an established technique for cross-sectional imaging in biomedical applications. OCT can also be used in the nondestructive evaluation of materials for industrial applications, although this promising field of applications is only partly exploited. There are two families of OCT systems:

- the Time Domain OCT (TD-OCT) which contains a sample arm in which a sample is illuminated with a broadband source and the backscattered light is collected and made to interfere with that from a reference arm [1]. The reference arm contains an optical delay line to continuously vary the depth at which the sample is probed.
- the Fourier Domain OCT (FD-OCT) where the signal is acquired as a function of the wavelength [2]. The depth profile of the sample is then achieved by computing the Fourier transform.

One of the key issues when imaging samples is to improve the depth resolution to see more and more details in the probed materials. Theoretically, the resolution is limited by the center wavelength of the source λ_0 and by its Full Width at Half Maximum (FWHM) $\Delta\lambda$. Indeed, for a source with a Gaussian shape the resolution in air is equal to:

$$\delta z = \frac{2\ln 2}{\pi}\frac{\lambda_0^2}{\Delta\lambda} \tag{1}$$

It means that in the case of a sample made of two close reflectors one cannot separate them if the space between each other is smaller than δz. One technique commonly used in ultrasonics to improve resolution for nondestructive evaluation is deconvolution

[3,4]. It consists in post-processing the signal taking into account the system response of a single reflector. Deconvolution has already been demonstrated in TD-OCT. Kulkarni et al. use a linear shift invariant system model [5] and Wang uses the Wiener filtering approach [6]. Both of them limited their studies to biological samples.

In the current paper, we present deconvolution algorithms based on Wiener filtering and Autoregressive Spectral Extrapolation (ASE) that are applied in both TD-OCT and FD-OCT. Firstly, we provide theoretical background for the proposed deconvolution algorithms. Secondly, we present the experimental setups used. Thirdly, the performance of the techniques is assessed by measurements on a glass wedge and the usefulness of the techniques is illustrated by thickness measurements of the upper layer of a carbon-epoxy composite.

DECONVOLUTION: THEORETICAL BACKGROUND

The signal *y(n)* collected by a TD-OCT system (or a FD-OCT system after data processing) can be simply modeled as the convolution between the point-spread function (PSF) *h(n)* and the reflector distribution *x(n)* in the sample:

$$y(n) = h(n) * x(n) \tag{2}$$

where n is the digitizer bin variable. The PSF corresponds to the system response to a single reflector. The goal is to recover the reflector distribution *x(n)* from the OCT signal. Without noise, the Fourier Transform *X(f)* of *x(n)* could be estimated using direct Fourier Transform as:

$$X(f) = \frac{Y(f)}{R(f)} \tag{3}$$

where f is the frequency, *R(f)* is the Fourier transform of *r(n)* the experimentally measured PSF of the system. By computing an inverse Fourier trasform, the reflector distribution *x(n)* is recovered and can be used for imaging.

The above procedure is simple but not efficient for a real signal in presence of noise. Two algorithms are used in this study to overcome this challenge. Let us consider a signal with N points and acquired with a sampling frequency f_s. The first algorithm is based on Wiener filtering and can be expressed as follow:

$$\overline{X}(k) = Y(k)\left[\frac{R(k)^*}{|R(k)|^2 + \chi^2 |R(k)|^2_{\max}}\right] \tag{4}$$

where $k=Nf/f_s$, $R(k)^*$ is the conjugate complex of $R(k)$, and χ^2 is a tunable factor, typically 0.01. The second algorithm is a wideband version of the Wiener filtering described above using Autoregressive Spectral Extrapolation (ASE). Formally, it is written as:

$$\begin{aligned}
\hat{X}(k) &= -\sum_{j=1}^{L} a_j^f \hat{X}(k-j) \quad \text{if } f \rangle f_{\max} \\
\hat{X}(k) &= -\sum_{j=1}^{L} a_j^b \hat{X}(k+j) \quad \text{if } f \langle f_{\min} \\
\hat{X}(k) &= \overline{X}(k) \qquad\qquad\quad \text{if } f_{\min} \langle f \langle f_{\max}
\end{aligned} \tag{5}$$

where the coefficients a_j^f and a_j^b are the L^{th} order forward and backward prediction coefficients. These coefficients are complex numbers and can be computed by using Burg's technique [7]. The order L is typically between 5 and 10.

EXPERIMENTAL SETUP

A TD-OCT system and a FD-OCT system are available in our institute. They are described below. Both of them are fiber-based OCT setups.

Time Domain OCT setup

The TD-OCT setup is shown in Fig. 1 and is based on a Michelson configuration. The source used in our experiment is a superluminescent diode (SLD) with a 1300 nm center wavelength and a 35 nm FWHM which leads to a theoretical depth resolution of $\delta z = 21.2$ µm. The light is split with a 2x2 coupler into the reference arm and the sample arm. The reference arm is fitted with a delay line which allows varying the optical path. The delay line is a galvanometer-mounted rhombic prism with a repetition rate of a hundred Hz, which has been used for many years in our institute. The backreflected light components from both arms are then combined into the coupler. The resulting interferometric signal is measured using balanced detection.

Fourier Domain OCT setup

Fourier Domain OCT has concentrated a lot of researchers' efforts in recent years. The two main advantages of this technique are that there is no moving part in the reference arm and that all the points of an A-scan are acquired simultaneously. In FD-OCT, the signal is collected as a function of the wavelength and two kinds of setup can be used. In the first one called Spectral Domain OCT (SD-OCT), a broadband source (SLED mainly) is used and the spectral interferogram is acquired by means of a spectrometer [2,8]. In the second one called Swept Source OCT (SS-OCT) [9], and also known as Optical Fourier Domain Imaging (OFDI) [10], a wavelength-swept source is used and the spectral interferogram is acquired with an InGaAs detector. The second setup is used in the current work (see Fig. 2).

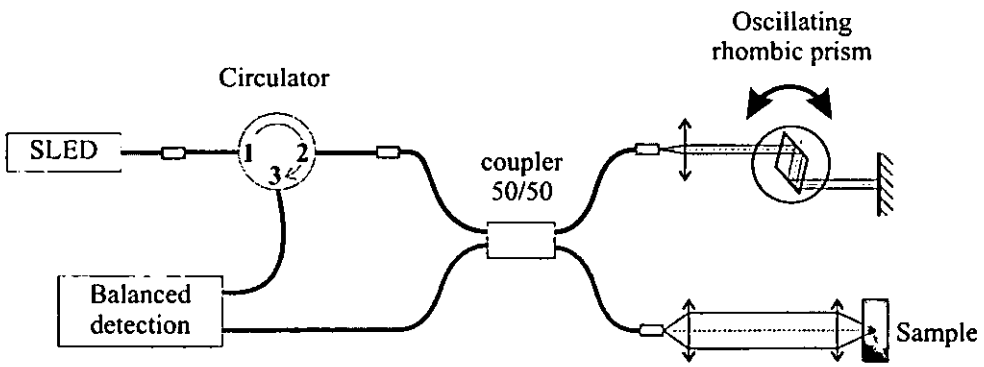

FIGURE 1. Time-Domain OCT setup.

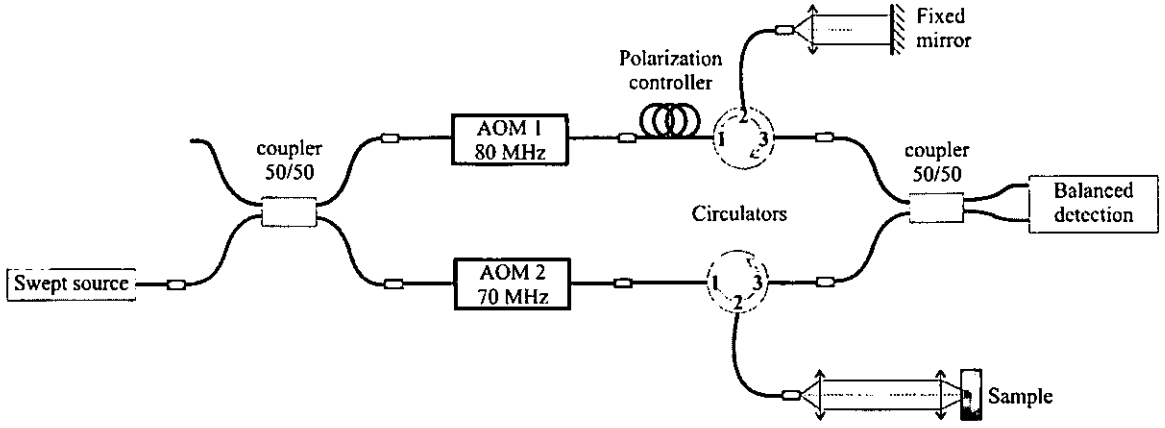

FIGURE 2. FD-OCT setup with a swept-source.

More precisely, our setup is a Mach-Zehnder fiber based interferometer. The source is a Thorlabs swept-source with a 1325 nm center wavelength and an 85 nm FWHM. The A-scan rate is 16 kHz. The theoretical axial resolution is then $\delta z = 9.1$ µm. The setup is fitted with acousto-optic modulators to remove the mirror image and autocorrelation noise generated by the computation of the Fourier Transform [11,12].

EXPERIMENTAL RESULTS

In this section, measurements have been taken with TD-OCT and FD-OCT setups. First, we show an example of resolution enhancement. Then, we present the approach to determine the resolution limit of our systems. Finally, measurements on a carbon-epoxy composite are presented.

Example of deconvolution results

A first illustration of the deconvolution methods is provided in Fig. 3 where a sample composed of two very close reflectors is considered. The envelope of the OCT signal does not enable us to separate these two reflectors (Fig. 3, upper right). After ASE deconvolution, the two reflectors can be clearly seen (Fig. 3, bottom right).

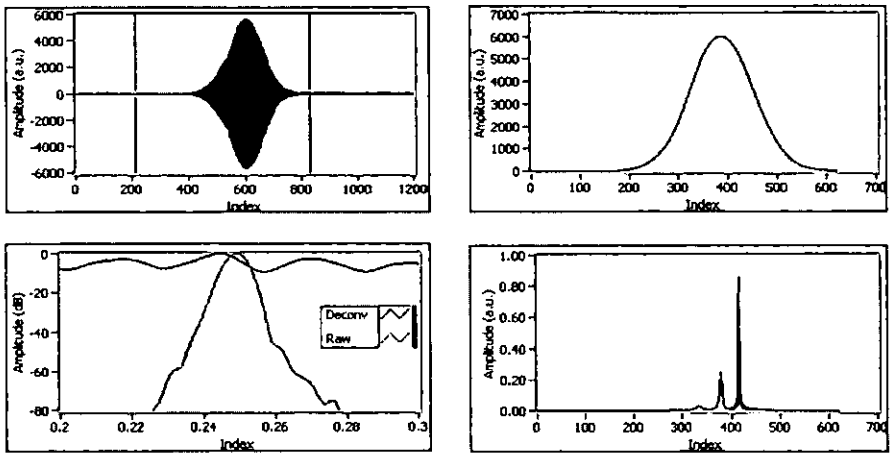

FIGURE 3. Example of resolution enhancement in TD-OCT using the ASE deconvolution technique for a separation of 5.9 µm between reflectors. Upper left: OCT signal, upper right: envelope of the OCT signal, bottom left: spectra of the raw and deconvoluted signals, bottom right: envelope of the deconvoluted data.

Resolution enhancement on a glass wedge

To determine the resolution limit of our system using deconvolution, we perform measurements on a sample that consists of two glass slides superimposed with a small angle as shown on the left in Fig. 4.

The separation between the two glass slides varies linearly as a function of the probe position. The reference signal used in the deconvolution is chosen where the separation is sufficient to capture a portion from a single reflector. The reference signal taken from the bottom of the top slide or from the top of the bottom slide gives about the same performance. The right of Fig. 4 shows the separation as a function of the probe position. Without deconvolution the minimum separation achievable is around 21 μm which corresponds to the expected theoretical resolution. With the Wiener filtering deconvolution, the separation decreases to 8 μm and with the ASE deconvolution, it reaches 5 μm. It means that, thanks to deconvolution, in our TD-OCT setup, the resolution is improved by a factor of at least 4.

In FD-OCT, we compute the inverse Fourier transform to get a signal equivalent to that of TD-OCT. It enables us to make a phase shifting on the complex TD-OCT signal in order to get an easier signal to process. Theoretically, after the phase shifting, the resulting shifted complex TD-OCT signal can be written as:

$$y_s = \mathrm{Re}\left[u[i]e^{j(2\pi\nu i)}\right] \tag{3}$$

where u[i] is the complex TD-OCT signal, ν is the phase shift coefficient. This approach is illustrated in Fig. 5.

The experimental resolution as a function of the probe position is given in the left part of Fig. 6. Without deconvolution it is about 12 μm. There is a noticeable difference between this measurement and the theoretical value of 9 μm. It is partly due to the fact that the swept-source spectrum does not have an exact Gaussian shape. Applying the Wiener filtering enables to achieve an 8 μm resolution. The maximum resolution obtained with the ASE deconvolution is around 6 μm. Therefore, an enhancement of a factor 2 is achieved in our FD-OCT setup.

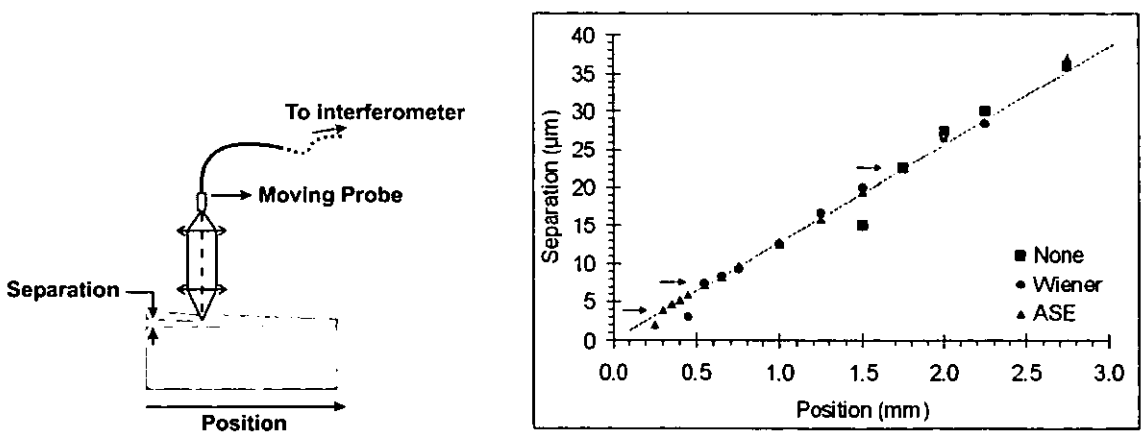

FIGURE 4. Resolution enhancement in TD-OCT. Left: experimental setup. Right: measured separation as a function of the lateral position on the probe (square: without deconvolution, circle: Wiener filtering, triangle: ASE).

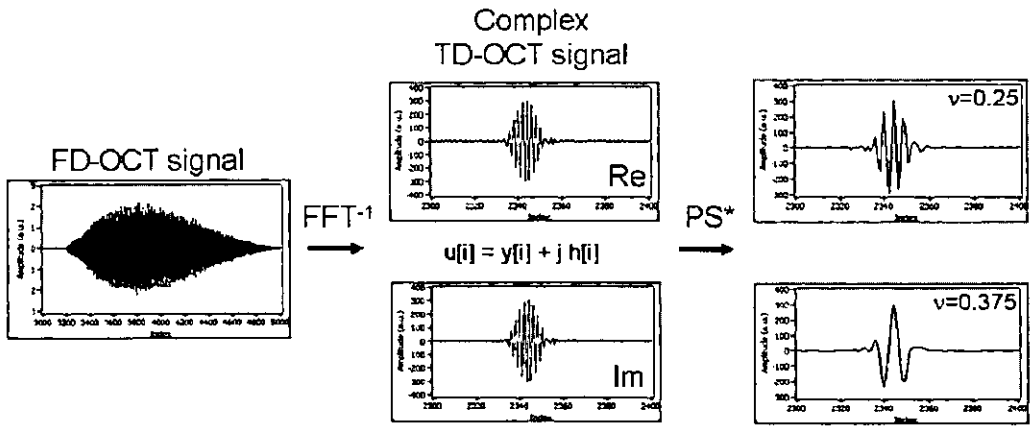

FIGURE 5. Pre-processing before applying the deconvolution. Firstly, the inverse Fourier transform is applied to the FD-OCT signal measured, and secondly, we apply a phase shifting to the result of this inverse Fourier transform.

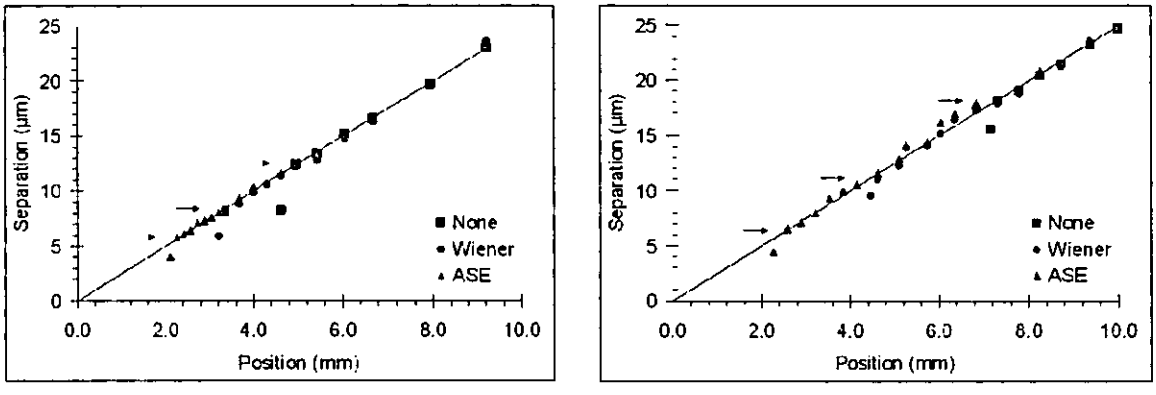

FIGURE 6. Resolution Enhancement in FD-OCT (square: without deconvolution, circle: Wiener filtering, triangle: ASE). Right: with the whole spectral range of the swept-source. Left: with a shorter spectral range.

As it seems that in both cases (TD-OCT and FD-OCT), the maximum resolution is around 5 µm, we artificially changed the resolution of our swept-source by selecting a shorter spectral range in the processing. These results are shown in the right part of Fig. 6. We get 18 µm without deconvolution. With Wiener filtering an 11 µm resolution is obtained and finally, we reach a 6.5 µm resolution with the ASE deconvolution. Therefore, this result suggests that whatever the initial resolution, the resolution limit after deconvolution is about the same.

The results of this section show that deconvolution enables enhanced resolution in both TD-OCT and FD-OCT.

Surface profile of carbon-epoxy composite

In this section, we apply the deconvolution algorithms to the determination of the epoxy layer of a carbon epoxy composite using OCT measurements. Our motivation to perform these measurements is that the layer thickness is of prime importance in laser-ultrasonic characterization. The thickness impacts the regime in which ultrasound is generated and thus determines the diffraction correction model to apply to laser-ultrasonic attenuation measurements [13].

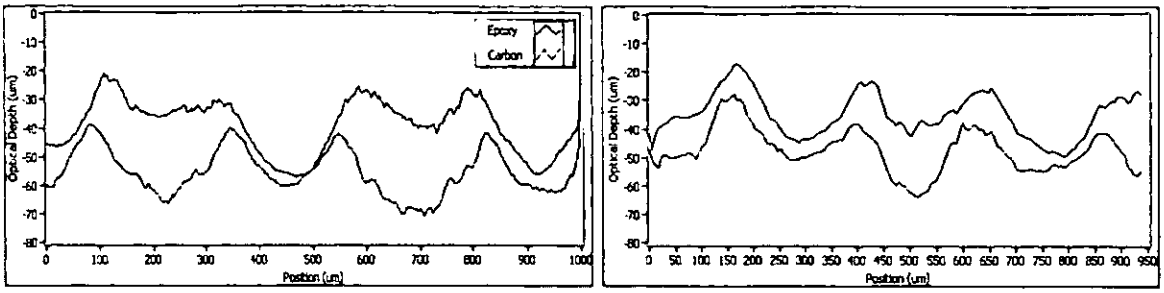

FIGURE 7. Surface profile of the carbon-epoxy composite in TD-OCT (left) and in FD-OCT (right). The probed areas are not the same in the two cases.

Once again, the measurements have been carried out in both TD-OCT and FD-OCT. The results achieved with the ASE algorithm are presented in Fig. 7. A moving average filter has been applied in these profiles to remove some noise. We see in each case that the epoxy layer is very well resolved. The presence of the individual carbon fiber is clearly seen as the epoxy layer is following more or less the same periodicity. It also provides the basic surface roughness of this material. Some depth differences between the two surfaces are lower than 10 μm in spite of the fact that the theoretical resolutions of our sources are larger than that. The deconvolution is therefore an efficient technique to improve resolution in TD-OCT and FD-OCT as well.

CONCLUSION

In this paper, a resolution enhancement was reported using deconvolution techniques in TD-OCT and FD-OCT as well. Two algorithms based on Wiener filtering and Autoregressive Spectral Extrapolation have been discussed. Actually, a resolution improvement of a factor 4 has been achieved in TD-OCT and of a factor 2 in FD-OCT. Moreover, in the case of FD-OCT, it seems that the resolution limit after deconvolution is independent of the initial resolution. To demonstrate the efficiency of the proposed techniques, the upper layer of a carbon-epoxy composite was well resolved. OCT appears to be a promising nondestructive evaluation technique for inspecting thin layered structures.

REFERENCES

1. D. Huang, E. A. Swanson, C. P. Lin et al., *Science* **254** (5035), pp. 1178-1181 (1991).
2. A. F. Fercher, C. K. Hitzenberger, G. Kamp et al., *Optics Communications* **117** (1-2), 43-48 (1995).
3. K. I. McRae, *Materials Evaluation*, pp. 1380-1384 (1990).
4. S.-K. Sin and C.-H. Chen, *IEEE Transactions on Image Processing* **1**, pp. 3-10 (1992).
5. M. D. Kulkarni, C. W. Thomas, and J. A. Izatt, *Electronics Letters* **33**, pp. 1365-1367 (1997).
6. R. K. Wang, *Journal of Modern Optics* **46**, pp. 1905-1912 (1999).
7. S. M. Kay, *Modern Spectral Estimation: Theory and Application*, Prentice Hall, (1988).
8. G. Hausler and M. W. Linduer, *Journal of Biomedical Optics* **3**, pp. 21-31 (1998).
9. S. R. Chinn, E. A. Swanson, and J. G. Fujimoto, *Optics Letters* **22**, pp. 340-342 (1997).
10. S. H. Yun, G. J. Tearney, J. F. de Boer et al., *Optics Express* **11**, pp. 2953-2963 (2003).
11. S. H. Yun, G. J. Tearney, J. F. de Boer et al., *Optics Express* **12**, pp. 4822-4828 (2004).

12. A. M. Davis, M. A. Choma, and J. A. Izatt, *Journal of Biomedical Optics* **10**, pp. 064005-064001 - 064005-064006 (2005).
13. B. Campagne, D. Lévesque, C. Bescond, C. Néron, A. Blouin and J.-P. Monchalin, "Laser-ultrasonic characterization of fiber reinforced composites: Effect of the generation laser transverse modes", in *Review of Progress in Quantitative Nondestructive evaluation Vol. 23*, ed. by D.O. Thompson and D.E. Chimenti, AIP Conf. Proc., New York (2004), pp. 302-309.